Proceedings of CONF-MPCS 2025 Symposium: Leveraging EVs and Machine Learning for Sustainable Energy Demand Management
DOI: 10.54254/2753-8818/109/2025.GL22980

High-frequency AlGaN/GaN T-gate HEMTs on SiC Substrate

Zilin Zheng

National University of Singapore, Kent Ridge, Singapore
zzlinus0157@gmail.com

Abstract: This paper investigates the DC and AC performance of T-gate Gallium Nitride (GaN) High Electron Mobility Transistors (HEMTs), with a particular emphasis on their high-frequency characteristics under various structure parameters and conditions. The study delves into the impact of different gate structures and the concentration of traps on the RF performance of the devices, including those at the AlGaN/GaN interface and within the GaN buffer layer. Moreover, the analysis includes the examination of short channel effects that can significantly influence the device behavior when the gate length is less than 100nm. Through comprehensive simulations, optimal structural parameters were identified, leading to notable advancements in device performance. Specifically, the devices achieved a remarkable cut-off frequency of 138 GHz and a maximum oscillation frequency of 192 GHz, accompanied by an extremely low gate leakage current, which is lower than 1E-8 mA/mm. These findings highlight the potential of T-gate GaN HEMTs in high-frequency applications.

Keywords: T-gate GaN HEMTs, Cut-off frequency, Maximum oscillation frequency.

1. Introduction

In modern electronics, the demand for higher frequency and higher power devices is driven by the need for more efficient power conversion, faster data processing, and enhanced performance in applications ranging from telecommunications to advanced computing systems. To meet these requirements, GaN HEMTs are becoming increasingly important due to their superior material properties compared to traditional Silicon based devices. As a wide bandgap semiconductor (Eg = 3.4 eV), GaN allows for higher breakdown voltages (4MV/cm) [1] and better performance in high-voltage environments, which is crucial for power electronics and RF devices where high voltage and power levels are necessary [2]. Furthermore, GaN HEMTs possess high electron mobility, resulting in faster switching speeds and higher frequencies of operation, which is particularly advantageous for RF and microwave applications [3]. They also exhibit better thermal stability and heat dissipation compared to Si devices, allowing for reliable performance under high-temperature conditions [4]. The robustness of GaN HEMTs makes them suitable for use in harsh environments such as space and military applications, as they can withstand radiation and high temperatures without significant performance degradation [5].

T-shape gate structure has been introduced to GaN HEMT to enhance the device's frequency performance. This is because T-shape gate can enhance the controllability to the channel without increasing the contact resistance [6]. M. Cho et al. developed a T-gate process for AlGaN/GaN-based fin-type HEMTs, achieving improved radio-frequency (RF) performance with a cut-off frequency of

DOI: 10.54254/2753-8818/109/2025.GL22980

9.7 GHz and a maximum oscillation frequency of 27.8 GHz, indicating a significant enhancement in RF capabilities due to the T-gate design [7]. Yeke Liu et al. demonstrated T-gate high-frequency AlGaN/GaN HEMTs on an extremely low resistivity silicon substrate, achieving cut-off frequency of 27 GHz, maximum oscillation frequency of 71 GHz, and a maximum transconductance of 247 mS/mm [8]. Jielong Liu et al. introduced millimeter-wave AlGaN/GaN MIS-HEMTs with Multiple T-gate technology, demonstrating superior frequency characteristics due to improved 2DEG mobility, which resulted in cut-off frequencies (f_t) of 87 GHz and maximum oscillation frequencies (f_{max}) of 158 GHz, showing the potential of T-gate structures on silicon substrates for RF application [9].

2. Device architecture

The structure of the device is illustrated in Figure 1. SiC is utilized as the substrate due to its high thermal conductivity. AlN layer serves as the nucleation layer to further reduce the lattice mismatch between the substrate and the GaN buffer layer. The Al content in the aluminum AlGaN barrier layer is 30%, which enhances both the piezoelectric polarization effect and the spontaneous polarization effect of the device. The GaN cap layer primarily acts as the surface layer of the device. By introducing surface donors to this layer, the two-dimensional electron gas (2DEG) beneath it can be modulated. The layer is doped to a concentration of 1E16/cm³ in the paper to enhance conductivity, which facilitates the formation of ohmic contacts.

Table 1 and Table 2 shows the device dimension and parameter used in simulation.

Table 1: Device dimension of T-gate GaN HEMT

Layer	Thickness	Length
Si3N4 passivation layer thickness	0.05μm	--
GaN cap layer	2nm	200nm
AlGaN barrier layer	11nm	200nm
GaN buffer layer	1.8μm	400nm
AlN nucleation layer	120nm	400nm
Source contact	67nm	100nm
Drain contact	67nm	100nm
T-gate head	5nm	120nm
T-gate foot	100nm	100nm

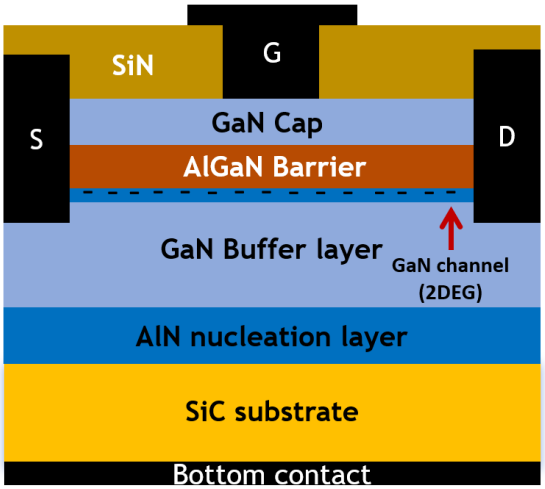

Figure 1: Schematic figure of T-gate GaN HEMTs for TCAD simulation

DOI: 10.54254/2753-8818/109/2025.GL22980

Table 2: Some important parameters of GaN and AlGaN used in simulation

Parameter	GaN	AlGaN
E_g@300K (eV)	3.4	3.9
Permittivity	9.4	9.4
N_c@300K (cm^{-3})	1E18	2E18
N_V@300K (cm^{-3})	1.18E18	1.18E18

3. Simulation approach

The device structure is defined and edited in the SDE. Specifically, the 5 nm GaN channel is designated as a separate region to facilitate subsequent modifications to model parameters. For the simulation of the device's electrical performance, the accurate selection of physical models is crucial for obtaining precise results. We selected the Doping Dependence Model and High Field Saturation Model for mobility. This choice is because wide-bandgap materials typically operate under high voltages, causing electrons to reach saturation velocity, deviating from the low-field rule ($v=\mu \cdot E$). The High Field Saturation Model accurately represents device behavior under these conditions. For the recombination model, we activated the SRH model and radiative model because the carrier concentration in the GaN HEMTs channel is very high, making recombination very important. The radiative model can effectively characterize the recombination in the quantum well, while the SRH can well represent the recombination phenomenon under high electron concentration. For the polarization phenomenon of GaN material, we activated a simple strain-based piezoelectric polarization model. We also activated the thermionic current model for electrons at a region-interface for heterojunction.

4. Results and discussion

Figure 2 (a) shows the output characteristics (I_D-V_D) curve of the T-gate GaN HEMT. As the applied gate voltage increases the maximum drain current increases. When V_G=2$V$and V_D=2.4V, the maximum drain current of the GaN HEMT can reach 1300 mA/mm. Figure 2 (b) shows the variation trend of the leakage current with changes in gate voltage. We can observe that when V_D=5V and V_G<1V, the drain current remains at a relatively low level.

Figure 2 (c) shows the transfer characteristics of (I_D-V_G) curve of the T-gate GaN HEMT at V_D=5V. The device's threshold voltage V_{th} is -2.07V. The transconductance (g_m) reaches its maximum value of 511.4 mS/mm. And from Equation 1, we can see that the cutoff frequency increases with the transconductance. As shown in Figure 2 (d), the cutoff frequency exhibits a trend similar to that of the g_m-V_G changes, reaching a peak value of 138 GHz at V_G=−0.65V.

$$f_t = \frac{g_m}{2\pi C_{gg}} \quad (1)$$

The relationship between f_{max} and V_G is shown in Figure 2 (e). In the region of higher gate voltage, since the device is already fully turned on, further increasing the gate voltage actually reduces f_{max}.

To further understand the impact of device structure on its RF performance, we next simulated devices with different parameters.

DOI: 10.54254/2753-8818/109/2025.GL22980

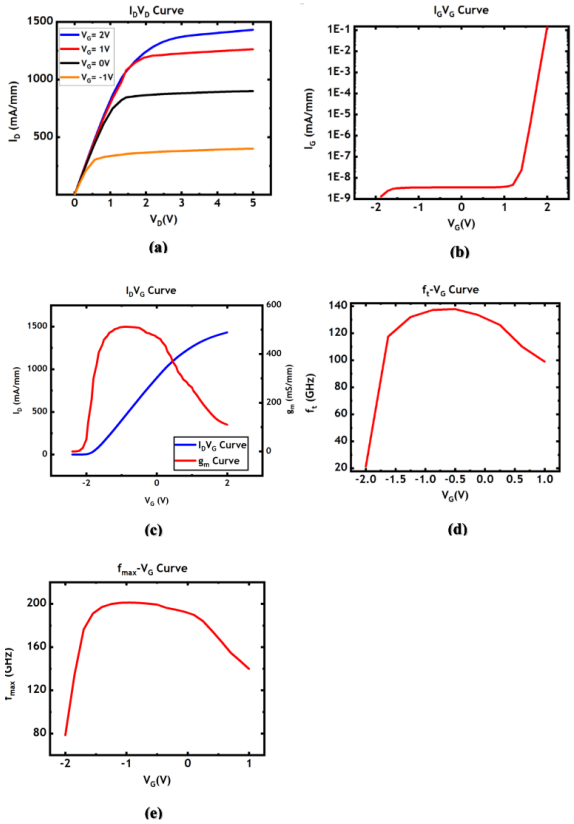

Figure 2: The (a) I_D-V_D curve; (b) I_G-V_G curve; (c) I_DV_G curve; (d) f_t-V_G curve and (e) f_{max}-V_G curve of T-gate GaN HEMT

The gate length typically affects the RF performance of the device. As shown in Figure 3 (a), an increase in gate length results in a decrease in transconductance. According to Equation 1, this leads to a corresponding decrease in cut-off frequency. Additionally, the increased gate length also raises the gate leakage current, which also reduces f_{max} of device.

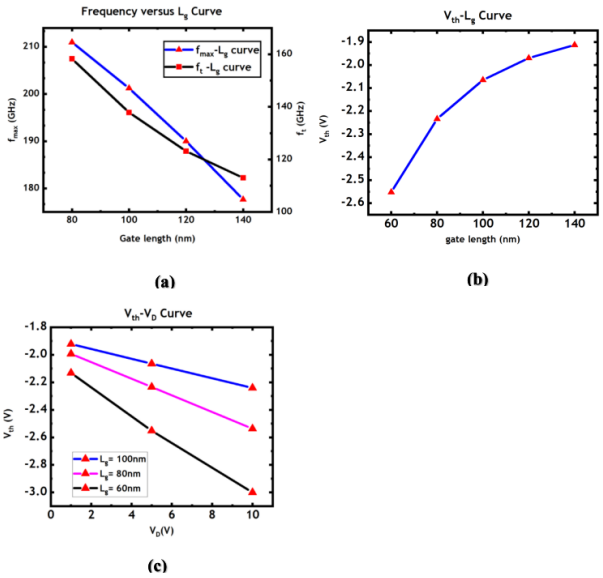

Figure 3: (a) maximum oscillation frequency amd cut-off frequency; (b) threshold voltage; (c) drain-induced barrier lowering effect of device with different gate length

DOI: 10.54254/2753-8818/109/2025.GL22980

However, shortening the gate length can cause short-channel effects. As shown in Figure 3 (b) and Figure 3 (c), when the gate length is less than 100 nm, noticeable V_{th} roll-off and drain-induced barrier lowering (DIBL) phenomena occur.

Traps are widely distributed throughout the device, primarily due to material defects, dopant atoms, lattice mismatch, and dangling bonds on the crystal surface. Additionally, deep-level traps (such as Fe doping) are intentionally introduced into the device to adjust the cutoff frequency and maximum oscillation frequency. These traps, due to electron capture effect, significantly affect the device's performance at high frequencies. Traps introduce in the paper is shown in Table 3.

Since the device's response to AC signals is based on electron migration between the GaN and AlGaN layers, AlGaN/ GaN interface traps can affect the high-frequency performance by influencing this migration. The impact of traps on electron capture can be seen in Figure 4 (a). When the trap concentration increases, the captured electron concentration also increases, resulting in a corresponding increase in the threshold voltage. Similarly, traps can also capture electrons leaking from the gate contact, thereby reducing gate leakage current, as shown in Figure 4 (b).

Table 3: The properties of two different types of traps in the device

Location of traps	AlGaN/GaN interface	GaN buffer layer
Distribution	Gaussian distribution	Uniform
Concentration	*C*GTrap cm−2 (at peak)	*N*tp cm−3
Type	Acceptor - like	Acceptor - like
Capture area	1E14 cm2	1E14 cm2

As illustrated in Figure 4 (c), an increase in trap concentration at the AlGaN/ GaN interface due to the capture effect makes it difficult for electrons to migrate from the AlGaN surface to the GaN layer in response to changing signals. This leads to a degradation in high frequency performance, including the cut-off frequency and maximum oscillation frequency. However, in the region of low trap concentration, the traps at the interface can also reduce gate leakage current, which results in a gradual increase in the maximum oscillation frequency.

Because GaN HEMTs use a 2DEG as their conductive channel, the electron concentration of the 2DEG is key to achieving high electron mobility. To enhance the spatial confinement of the 2DEG, an effective method is to introduce deep-level traps in the GaN buffer layer. The trend of the device's high-frequency performance with varying trap concentration in the GaN buffer layer is shown in Figure 4 (d). It can be seen that as the trap concentration increases, the 2DEG is confined to a very thin layer, increasing the electron concentration in the channel. This, in turn, improves the device's cut-off frequency and maximum oscillation frequency.

DOI: 10.54254/2753-8818/109/2025.GL22980

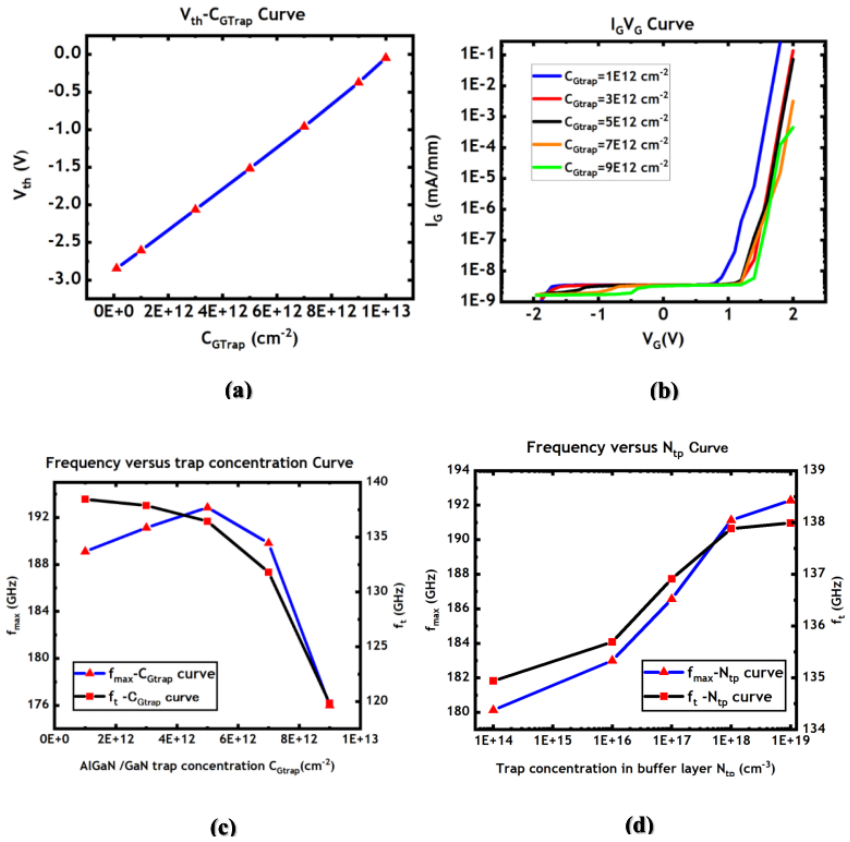

Figure 4: The (a) threshoald voltage; (b)I_G-V_G curve; (c) cut-off frequency and maximum oscillation frequency as a function of interface traps concentration and (d) cut-off frequency and maximum oscillation frequency as a function of traps concentration in GaN buffer layer

5. Conclusion

In this paper, DC and AC characteristics have been investigated for T-gate GaN HEMTs. The device exhibits a maximum drain current exceeding 1300 mA/mm, with a peak transconductance of 511.4 mS/mm and a gate leakage current below 1E-8 mA/mm. We also compare the frequency performance of our device with other papers, as shown in Figure 5, [8,10-13] and it can be seen that the GaN HEMTs in the paper have both high cutoff frequencies and high maximum oscillation frequencies.

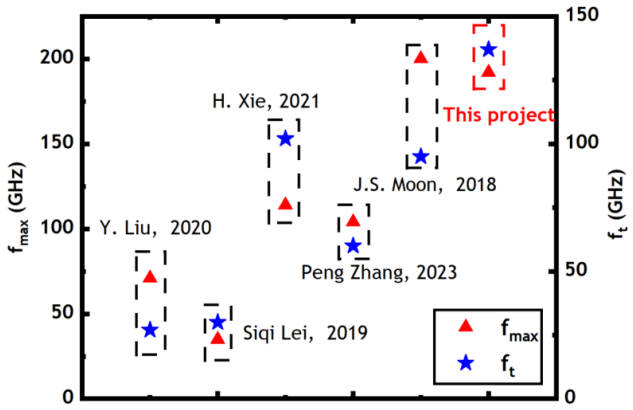

Figure 5: Comparation of GaN HEMTs frequency performance between our project and other paper

DOI: 10.54254/2753-8818/109/2025.GL22980

References

[1] M. S. Adler, K. W. Owyang, B. J. Baliga, and R. A. Kokosa, 'The evolution of power device technology', IEEE Trans. Electron Devices, vol. 31, no. 11, pp. 1570–1591, Nov. 1984, doi: 10.1109/T-ED.1984.21754.

[2] U. K. Mishra, L. Shen, T. E. Kazior, and Y.-F. Wu, 'GaN-Based RF Power Devices and Amplifiers', Proc. IEEE, vol. 96, no. 2, pp. 287–305, Feb. 2008, doi: 10.1109/JPROC.2007.911060.

[3] W. Johnson and E. L. Piner, 'GaN HEMT Technology', in GaN and ZnO-based Materials and Devices, S. Pearton, Ed., Berlin, Heidelberg: Springer, 2012, pp. 209–237. doi: 10.1007/978-3-642-23521-4_7.

[4] X. Cai et al., 'Recent progress of physical failure analysis of GaN HEMTs', J. Semicond., vol. 42, no. 5, p. 051801, May 2021, doi: 10.1088/1674-4926/42/5/051801.

[5] T. Satoh, K. Osawa, and A. Nitta, 'GaN HEMT for Space Applications', in 2018 IEEE BiCMOS and Compound Semiconductor Integrated Circuits and Technology Symposium (BCICTS), Oct. 2018, pp. 136–139. doi: 10.1109/BCICTS.2018.8551070.

[6] J. Shao, J. Deng, W. Lu, and Y. Chen, 'Nanofabrication of 80 nm asymmetric T shape gates for GaN HEMTs', Microelectron. Eng., vol. 189, pp. 6–10, Apr. 2018, doi: 10.1016/j.mee.2017.12.001.

[7] M. S. Cho, J. H. Seo, S. H. Lee, H. S. Jang, and I. M. Kang, 'Fabrication of AlGaN/GaN Fin-Type HEMT Using a Novel T-Gate Process for Improved Radio-Frequency Performance', IEEE Access, vol. 8, pp. 139156–139160, 2020, doi: 10.1109/ACCESS.2020.3011103.

[8] Y. Liu, C.-H. Li, W.-C. Hsu, C.-Y. Chuang, J.-Z. Liu, and S. S. H. Hsu, 'High-frequency AlGaN/GaN T-gate HEMTs on extreme low resistivity silicon substrates', Jpn. J. Appl. Phys., vol. 59, no. SG, p. SGGD11, Feb. 2020, doi: 10.35848/1347-4065/ab70a5.

[9] J. Liu et al., 'Millimeter-Wave AlGaN/GaN MIS-HEMTs with Multiple T-Gate Technology', in 2023 IEEE International Conference on Integrated Circuits, Technologies and Applications (ICTA), Oct. 2023, pp. 1–2. doi: 10.1109/ICTA60488.2023.10364256.

[10] S. Lei et al., 'Low leakage GaN HEMTs with sub-100 nm T-shape gates fabricated by a low-damage etching process', J. Mater. Sci. Mater. Electron., vol. 31, no. 8, pp. 5886–5891, Apr. 2020, doi: 10.1007/s10854-019-02758-z.

[11] H. Xie, Z. Liu, Y. Gao, K. E. Lee, and G. I. Ng, '100 nm T-gate GaN-on-Si HEMTs Fabricated with CMOS-Compatible Metallization for Microwave and mm-Wave Applications', in 2021 5th IEEE Electron Devices Technology & Manufacturing Conference (EDTM), Apr. 2021, pp. 1–3. doi: 10.1109/EDTM50988.2021.9420941.

[12] P. Zhang, M. Li, J.-W. Chen, J.-Z. Liu, and X.-H. Ma, 'Research on self-supporting T-shaped gate structure of GaN-based HEMT devices', Chin. Phys. B, vol. 32, no. 6, p. 067305, Jun. 2023, doi: 10.1088/1674-1056/acaa27.

[13] J. s. Moon, R. Grabar, M. Antcliffe, H. Fung, Y. Tang, and H. Tai, 'High-speed FP GaN HEMT with fT/fMAX of 95/200 GHz', Electron. Lett., vol. 54, no. 10, pp. 657–659, 2018, doi: 10.1049/el.2018.0417.